Journal of Materials Chemistry B

Accepted Manuscript

ROYAL SOCIETY OF CHEMISTRY

www.rsc.org/materialsB

Journal Name

RSCPublishing

ARTICLE

Antifouling property of monothiol-terminated bottle-brush poly(methylacrylic acid)-graft-poly(2-methyl-2-oxazoline) copolymer on gold surfaces

Cite this: DOI: 10.1039/xoxxoooooox

Received ooth January 2012,
Accepted ooth January 2012

DOI: 10.1039/xoxxoooooox

www.rsc.org/

Xiajun Zheng, Chong Zhang, Longchao Bai, Songtao Liu, Lin Tan, Yanmei Wang*

In this study, a series of well-controlled bottle-brush polymers, poly(methylacrylic acid)-g-poly(2-methyl-2-oxazoline) with monothiol-terminated group ((PMAA-g-PMOXA)-SH) were synthesized by using reversible addition-fragmentation chain transfer (RAFT) polymerization and cationic ring-opening polymerization (CROP), and then (PMAA-g-PMOXA)-SH were grafted to the surface of gold sensor in situ aminolysis reaction. Cyclic voltammetric (CV), X-ray photoelectron spectroscopy (XPS), variable angle spectroscopic ellipsometry (VASE), water contact angle (CA) and atomic force microscopy (AFM) were used to characterize the copolymer modified gold sensor. The protein resistant property was investigated by surface plasmon resonance (SPR). And platelet adhesion was observed by scanning electron microscopy (SEM). Compared with the bare gold sensor, the ($PMAA_{20}$-g-$PMOXA_{12}$)-SH modified gold sensor can reduce the levels of fibrinogen (Fg), bovine serum albumin (BSA) and lysozyme (Lyz) adsorption by 96.5±3.1% , 85.8±5.7%, and 49.4±1.6%, respectively. Meanwhile, the ($PMAA_{20}$-g-$PMOXA_{12}$)-SH modified gold sensor also possess excellent resistance to platelet adhesion. All these data demonstrated that this simple method is feasible, and bottle-brush (PMAA-g-PMOXA)-SH modified gold sensor has potential application in biosensor and biomedical areas.

Introduction

Nowadays, gold is extensively applied in biosensor interfaces, such as electrochemical biosensors,[1] surface plasmon resonance (SPR)[2,3] and quartz crystal microbalance (QCM),[4] because of its many prominent property, such as hard to oxidation, better conductivity and easy for surface modification.[5-8] In particular, a biosensor made of gold applied to the clinical diagnosis of epidemic diseases,[9] long-term nursing of chronic diseases,[10] and early diagnosis of cancers[11] can save many lives around the world. Whereas, when the gold biosensor exposed to complex biological fluids environment, a series of harmful responses including thrombus formation, blood coagulation, platelet activation and other unfavorable responses have occurred,[12-14] which resulting in a low signal-to-noise ratio (S/N),[15, 16] leading to low biosensor efficiency. All these consequences are considered due to the protein fouling on the substrate surfaces once the substrate contact with the biological fluids. Therefore, rendering the protein resistant property to biosensor is of a matter of debate in the development of biosensor areas. The grafting of antifouling materials to the substrate surface is a general method.

It is widely known that poly(ethylene glycol) (PEG), oligo(ethyleneglycol) (OEG) and their derivatives have been extensively used as antifouling materials and show excellent antifouling property.[17-19] However, PEG is known to undergo degradation by (auto-) oxidation to form aldehydes and ethers which limiting their application.[20] Furthermore, PEG coatings will lose their function when paced in vivo.[21, 22] Thus, it is necessary to search for the alternative polymers. In recent years, poly(2-oxazoline)s appear in researchers' field of vision, especially the water soluble poly(2-methyl-2-oxazoline) (PMOXA) as biomaterials owing to its many distinctive properties, such as tolerating to oxidative degradation,[23] a less demanding synthesis[24] and non-cytotoxicity.[25] Furthermore, it is reported that substrate surfaces modified with poly(2-oxazoline)s have shown similar protein-repellent properties to PEG based materials.[26,27] In the past decades, several approaches have been applied to tether the polymer on solid substrate such as "grafting to",[28, 29] and "grafting from"[30-32] etc. Although the "grafting from" approach can produce polymer brushes on the substrate with high grafting density, the requirements of functionalized surface and inert polymerization conditions make it difficult for preparing antifouling

surface. Additionally, the living cationic ring-opening polymerization (CROP) used for PMOXA polymerization must be performed strictly within an inert atmosphere as it is sensitive to oxygen and water. Therefore, the most common used method for anchoring PMOXA is "grafting to" method. Recently[27], a simple annealing protocol has been used to graft the comb copolymer poly [(2-methyl-2-oxazoline)-random-glycidyl methacrylate] (PMOXA-r-GMA) onto the silicon/glass to yield a covalent and cross-linked PMOXA-based antifouling coating in our group. The aim of this work is to deal with the biofouling problem on gold substrates which have been extensively applied in electrochemical biosensors[1], SPR[2, 3], QCM[4] and other biosensor and biomedical areas. When it refer to antifouling property, some researches have shown that bottle-brush polymers are the kind attractive candidate for antifouling coating due to their conformational flexibility and high grafting density of the side chains.[33-35] Zhang and coworkers[36] have prepared some poly(2-oxazoline)s based bottle-brush brushes on amino-functionalized silicon/silicon dioxide substrates via a two-step polymerization using "grafting from" method, and found these kinds of coatings possess an excellent non-fouling behavior while the bottle-brush brushes are composed with poly(2-methyl-2-oxazoline) side chains. Thus we believe that tethering the PMOXA with bottle-brush structure to the gold substrate using the "grafting to" method will produce a good antifouling coating.

Ulrich S. Schubert and coworkers have reported that the bottle-brush polymers composed of a poly(methylacrylic acid) (PMAA) backbone and oligo (2-ethyl-2-oxazoline) (OEtOx) side chains can be synthesized by using living OEtOx chains directly grafting onto a deprotonated PMAA backbone.[37] Motivated by this, we synthesized a series of graft polymers composed of PMAA backbone and PMOXA side chains in this work. As illustrated in Scheme 1, firstly, PMAA backbone were synthesized using the reversible addition-fragmentation chain transfer (RAFT) polymerization and PMOXA side chains were obtained by cationic ring-opening polymerization (CROP) of methy oxazoline (MOXA), and then the living oligomeric oxazolinium species were terminated by deprotonation PMAA to obtain bottle-brush PMAA-g-PMOXA with a dithioester group. As it is known, gold has a strong specific interaction with thiol,[38,39] so the polymers terminated with a dithioester can be conferred into thiol-terminated ((PMAA-g-PMOXA)-SH) by aminolysis,[40-43] and then bonded to the gold surface. Whereas the susceptibility of thiol to aerial oxidation (to form the corresponding disulfide) is also a potential problem using thiol. In order to minimize this problem, firstly, bare gold sensor was immersed into dithioester terminated polymer solution, and then the bottle-brush polymer can be anchored to the gold substrate to form bottle-brush coating through thiol group generated during situ aminolysis in this work. The protein resistant properties of the bottle-brush (PMAA-g-PMOXA)-SH coatings could be finely tuned by varying the backbone and side chain length. Protein adsorption was analyzed quantitatively by using surface plasmon resonance (SPR) performed with fibrinogen (Fg), bovine serum albumin (BSA) and lysozyme (Lyz). And platelet adhesion was observed by scanning electron microscopy (SEM).

Experiment section

Materials

SPR gold sensors were used as the substrate. Triethylamine (TEA), 2-methylacrylicacid (MAA), N, N-dimethylformamide (DMF), diethyl ether, chloroform, 2-aminoethanol (MEA), acetonitrile (AN), ethanol, CaH_2, 2, 2'-dicyano-2,2'-azopropane (AIBN), were purchased from Sinopharm Chemical Reagents Co., Ltd. (SCRC, Shanghai, China), and purified according to standard methods before use. 4-Cyanopentanoic acid dithiobenzoat (CPDB) was synthesized according to the literature procedure.[44] 2-Methyl-2-oxazoline (MOXA, Aldrich, 98%) was dried by CaH_2 overnight, and then distilled before use. Methyl p-toluenesulfonate (MeOTs) was purchased from Aldrich and used as received. Fibrinogen (Fg, 340 kDa, pI = 5.5), bovine serum albumin (BSA, 66 kDa, pI = 4.7), and lysozyme (Lyz, 14 kDa, pI = 12) were purchased from Sigma-Aldrich. All water used in this experiment was deionized water.

RAFT polymerization of PMAA

MAA (3.00 g, 34.88 mmol) was dissolved in 2.50 mL ethanol, and AIBN (71.50 mg, 0.44 mmol) in 2.00 mL ethanol as well as a solution of CPDB (385.42 mg, 1.74 mmol) in ethanol (4.00

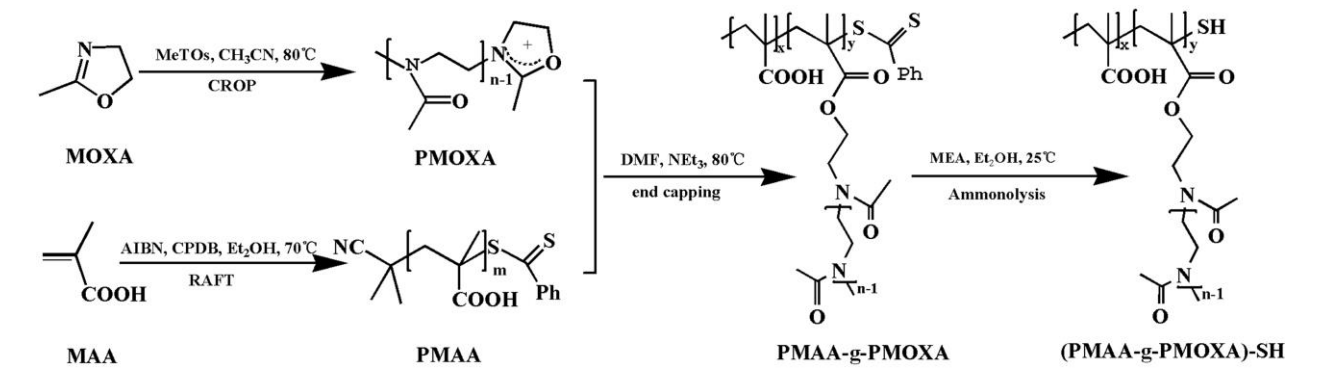

Scheme 1 Schematic illustration of the synthesis and structure of (PMAA-g-PMOXA)-SH polymer.

mL) were added into a round bottom flask with a magnetic stirring bar, then other 8.94 mL ethanol were added. The concentration of monomer was 2.00 mol L^{-1} and the ratio of [monomer] : [CPDB] : [AIBN] was 20 : 1 : 0.25. After three freeze-pump-thaw cycles, the flask was flame sealed under vacuum. And then the flask was placed in a 70 ℃ oil bath. After 15 h, the reaction flask was quenched by an ice-water bath. Then the crude product was precipitated into chloroform. The resulted pink powder were obtained by dialysis (membrane 1000 Da molecular weight cutoff) against deionized water for 3 days and then lyophilized. The obtained polymer using above recipe was named as $PMAA_{20}$. Another polymer $PMAA_{40}$ was synthesized in the same process only by changing the [monomer] : [CPDB] molar ratios to 40.

Synthesis of (PMAA-g-PMOXA)-SH

MOXA (4.43 mL, 52.30 mmol), MeOTs (0.66 mL, 4.40 mmol), AN (8.86 mL) were added to a 25 mL Schlenk tube under a nitrogen atmosphere. The polymerization was performed at 80°C for 22 h. After that, $PMAA_{20}$ (0.20 g) and TEA (0.49 mL) which dissolved in DMF (0.87 mL) in advance under the protection of nitrogen were added to the Schlenk tube, then the tube were heated to 80 °C for 24 h. After that, the solution was quenched by using an ice-water bath. The resulting products were obtained by precipitation into diethyl ether. With purification, the obtained polymers were dialyzed (membrane 3500 Da molecular weight cutoff) in deionized water for 3 days and then lyophilized. The color of the product was pink. We defined this polymer as $PMAA_{20}$-$PMOXA_{12}$. Similarly, another two copolymer $PMAA_{20}$-$PMOXA_6$ and $PMAA_{40}$-$PMOXA_6$ with different backbone and different side chain length were synthesized using the same procedure as above by solely changing the MOXA/MeOTs molar ratios from 12 : 1 to 6 : 1. While the MOXA monomer was always 1/2 of the AN solvent. Partial resulting copolymer was converted to the thiol terminated polymer ((PMAA-g-PMOXA)-SH) by aminolysis with MEA (MEA to polymer = 20 : 1) for further characterization. A typical procedure is as follows. $PMAA_{20}$-$PMOXA_{12}$ (0.50 g) was dissolved in 20 mL deionized water and then the polymer solution was added into a three necked, round bottom flask equipped with a Teflon coated magnetic stir bar. After that, 20 mol equiv MEA were added to the polymer solution. The reaction mixture was deoxygenated by bubbling with nitrogen. The solution was then stirred at ambient temperature for 4 h until the polymer solution became colorless. And then ($PMAA_{20}$-$PMOXA_{12}$)-SH was obtained after purification the polymer solution by dialysis in deionized water for 3 days and lyophilization. ($PMAA_{20}$-$PMOXA_6$)-SH and ($PMAA_{40}$-$PMOXA_6$)-SH were obtained as the same process.

Preparation of polymer-modified gold SPR sensors

The gold SPR sensors were glass slides coated with an adhesion-promoting chromium layer (thickness 5 nm) and a surface plasmon-active gold (Au) layer (45 nm) by electron beam evaporation under vacuum. Before polymer coating, the SPR sensors were immersed into freshly prepared piranha solution (H_2SO_4 : H_2O_2 = 3 : 1, v/v, 70°C) for 10 min to remove any organic contamination, and then rinsed with deionized water and ethanol and dried under a stream of nitrogen. The preparation process is showed in Scheme 2. The polymer solutions were prepared by dissolving PMAA-g-PMOXA into ethanol at room temperature to keep the polymer solution concentration 5 mg/mL. Then MEA were added to the polymer solution, maintaining the molar ratio of MEA to polymer at 20 : 1. The reaction mixture was deoxygenated by bubbling with nitrogen, and then freshly prepared gold sensors were immersed in and shaken in an orbital shaker for 48 h at room temperature. After that the modified gold sensors were washed with deionized water and ethanol to remove unbonded polymer and dried in a nitrogen stream.

The characterization of copolymer

NMR spectroscopy

^1H NMR spectra were recorded on a Bruker AV300 NMR spectrometer (resonance frequency of 300 MHz for ^1H) operated in the Fourier transform mode. Deuterated dimethyl sulfoxide (DMSO) was used as the solvent.

Gel permeation chromatography (GPC)

The polydispersity indices (PDI) of PMAA and (PMAA-g-PMOXA)-SH were determined by GPC. GPC of PMAA was performed by a Waters gel permeation chromatography analysis system equipped with four Ultrahydrogel columns (2000, 500, 250 and 120; 7.8×300 mm), the column temperature was 35°C. The mobile phase employed was phosphate buffer saline (pH=7.4) at a rate of 1 mL/min calibrated with PEO standards. As for (PMAA-g-PMOXA)-SH copolymers, tandem gel permeation chromatography/light scattering (GPC/LLS) was performed at 50 ℃ using a SSI pump connected to Wyatt Optilab DSP and Wyatt DAWN EOS light scattering detectors with DMF containing 0.02 mol/L LiBr salt as eluent at a flow rate of 1.0 mL/min, and separations were achieved using 10^5, 10^4, and 10^3 Å Phenomenex Phenogel 5 μm columns.

UV-vis absorption spectra

UV-vis absorption spectra were taken on a Shimadzu UV-2550 spectrophotometer using 1-cm path length quartz cuvettes. Ethanol was used as the solvent.

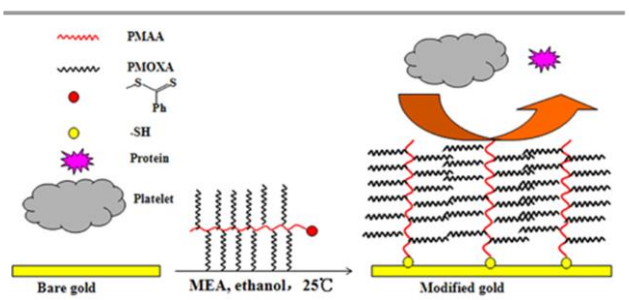

Scheme 2 Modification route of gold sensor.

The characterization of copolymer-modified SPR sensors

Electrochemical measurements

The cyclic voltammetric (CV) studies were performed by using a CHI600D electrochemical workstation (Chenhua, Shanghai) with a three-electrode system of platinum wire as a counter electrode and Ag/AgCl as a reference electrode. The barrier properties of unmodified and modified gold sensors were evaluated in a solution of ferricyanide (10 mM) ($[Fe(CN)_6]^{3-}$/$[Fe(CN)_6]^{4-}$) contained 0.1 mol L^{-1} KCl. The potential window was −0.2 to 0.6 V and then 0.6 to −0.2 V (*vs.* Ag/AgCl), and the scanning rate was 100 mV/s.

Variable-angle spectroscopic ellipsometry (VASE)

The variable-angle spectroscopic ellipsometry (VASE) spectra were carried out on a spectroscopic ellipsometer (M-2000, Woollam Co., Inc., Lincoln, NE). The measurements were performed in the spectral range of 370-1000 nm at two different angles of incidence (70 °and 80 °). The analysis software CompleteEASE 4.81 was used to analyze all data. A Cauchy layer model was used to determine film thickness. In order to ensure the formation of homogeneous polymer coating, every sample was measured at least three times.

Atomic force microscopy (AFM)

The surface morphologies of polymer-coated gold sensors were determined by using atomic force microscope (AFM) (Veeco Instruments, Mannheim, Germany) with tapping mode in dry state. Measurements were performed in air.

Contact angle measurements

Wettability of the modified sensors was investigated with a Kino SL200K instrument (America), using the sessile drop method under room temperature. A water drop with volume of 2 uL was dropped onto the samples with a microsyringe in an atmosphere of air. At least 3 contact angles at different locations on each sample were measured to get a reliable value.

Protein adsorption experiments

Protein adsorption was measured with a BIACORE 3000 system instrument (Sweden BIACORE AB) for SPR study at room temperature. Protein adsorption on a modified SPR sensor and unmodified SPR sensor was tested with Fg, BSA, and Lyz in PBS buffer (137 mM NaCl, 2.7 mM KCl, 2 mM KH_2PO_4 and 10 mM Na_2HPO_4, pH 7.4). A baseline signal was established by flowing PBS buffer at a rate of 0.05 mL/min through the sensor until the baseline being stable. 1 mg/mL single-protein solution of Fg, BSA, Lyz flowed through independent channels for 10 min, and then the channels were rinsed with PBS buffer solution to remove unbound protein molecules. The amount of adsorbed proteins on the surface was quantified by measuring wavelength change (1000 RU=1 ng/mm^2) between the baselines before and after protein injection.

Platelet adhesion

The gold sensors were placed in individual wells of 6-well tissue culture plate and equilibrated with PBS for 2 h. Fresh blood with 3.8% sodium citrate anticoagulant (9:1) was centrifuged (1200 rpm, 10 min) to obtain platelet-rich plasma (PRP). And then the bare gold sensor and modified gold sensor were incubated with PRP for 2 h at 37 ℃. After being rinsed with PBS, the substrates were immersed into 2.5% glutaraldehyde in PBS for 30 min, subjected to a series of graded alcohol–water solutions (25%, 50%, 75%, 95% and 100%) for 20 min in each step and dried under vacuum. Finally, the substrates were examined by a scanning electron microscope (SIRION200, FEI, USA).

Results and discussion

Synthesis of monothiol-terminated bottle-brush copolymer

The chemical structure and synthesis route of monothiol terminated (PMAA-g-PMOXA)-SH are shown in Scheme 1. Dithiobenzoate group terminated PMAAs were synthesized use RAFT polymerization. Then PMOXA side chains were introduced using the deprotonated PMAA backbone to terminate the PMOXA cation species. Subsequently, the thiol terminated polymers were obtained by aminolysis with MEA. Three samples $PMAA_{40}$-g-$PMOXA_6$, $PMAA_{20}$-g-$PMOXA_6$ and $PMAA_{20}$-g-$PMOXA_{12}$ with different structure varying backbone and side chain length were prepared. Fig. 1 shows the ^{1}H NMR spectra of $PMAA_{20}$ (in black of Fig. 1(a)), $PMAA_{40}$ (in red of Fig. 1(a)), $PMAA_{40}$-g-$PMOXA_6$ (in black of Fig. 1(b)), $PMAA_{20}$-g-$PMOXA_6$ (in red of Fig. 1(b)), and $PMAA_{20}$-g-$PMOXA_{12}$ (in green of Fig. 1(b)). All of the corresponding resonance peaks (a, b, c, d) of PMAA were found in the spectra. As shown in Fig. 1(a), comparing the peak integrals of $PMAA_{20}$ (in black) and $PMAA_{40}$ (in red) derived from the carboxyl protons (d) at 12-13 ppm with the aromatic proton (c) at 7.4−8.2 ppm, respectively, the degree of polymerization (DP) of $PMAA_{20}$ and $PMAA_{40}$ were 22.25 and 43.90 individually. The GPC data of $PMAA_{20}$ and $PMAA_{40}$ were shown in ESI (Table S1 and Fig. S1). The PMAAs with relatively low polydispersity (PDI<1.2) were obtained, suggesting the living characteristics of the RAFT polymerization process. The chemical shifts of all the protons in the copolymers can be clearly identified in Fig. 1(b), attesting to the formation of the expected structures. The peak around 7.4−8.2 ppm in Fig. 1(b) was assigned to aromatic proton c. Peaks a and b were attributed to PMAA characteristic peak. The e, f, g, h proton peaks from MOXA side chains indicated the inclusion of PMOXA and PMAA moieties in the polymer. The content of PMOXA in the copolymers was calculated from the ^{1}H NMR data as follows:

$$PMOXA(mol\%) = \frac{I_f/3}{I_a/3} \times 100$$

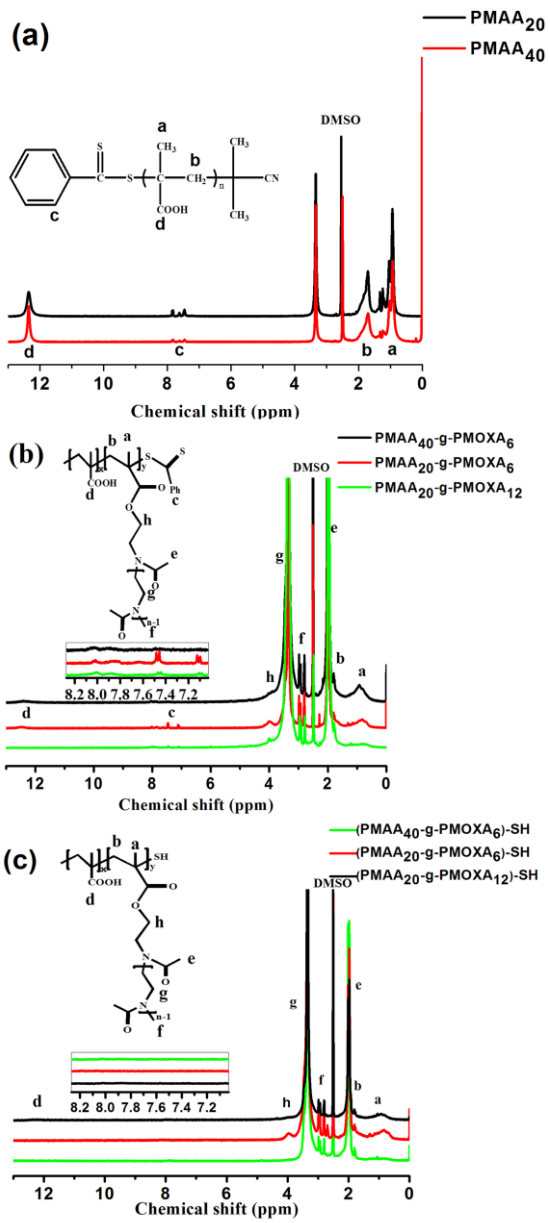

Fig. 1 ^{1}H NMR spectra (300 MHz, DMSO-d_6) of PMAA with different DP (a), $PMAA_{40}$-g-$PMOXA_6$, $PMAA_{20}$-g-$PMOXA_6$, $PMAA_{20}$-g-$PMOXA_{12}$ (b) and ($PMAA_{40}$-g-$PMOXA_6$)-SH, ($PMAA_{20}$-g-$PMOXA_6$)-SH, ($PMAA_{20}$-g-$PMOXA_{12}$-SH) (c).

where I_a and I_f are the intensities of the a and f proton peaks, respectively (Fig. 1b). The content of PMOXA in the copolymers of $PMAA_{40}$-g-$PMOXA_6$, $PMAA_{20}$-g-$PMOXA_6$, and $PMAA_{20}$-g-$PMOXA_{12}$ is 86.9%, 85.4% and 83.3%, respectively. The DP of PMOXA side chain can be calculated from the integral ratio of methyl protons (Fig. 1(b)-e) and methyl protons (Fig. 1(b)-f). The DP of PMOXA side chains in $PMAA_{40}$-g-$PMOXA_6$, $PMAA_{20}$-$PMOXA_6$, and $PMAA_{20}$-g-$PMOXA_{12}$ were about 4.72, 4.77, and 10.36, respectively. And the GPC data of ($PMAA_{40}$-g-$PMOXA_6$)-SH, ($PMAA_{20}$-$PMOXA_6$)-SH and ($PMAA_{20}$-g-$PMOXA_{12}$)-SH were

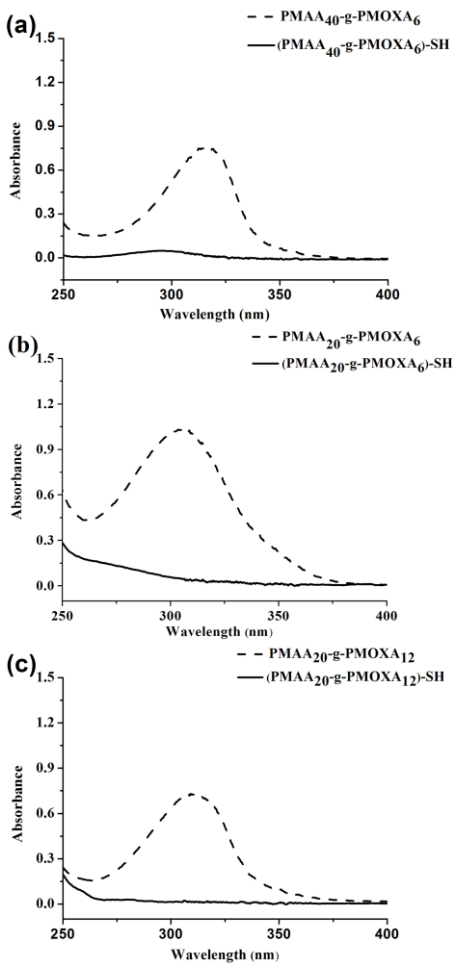

Fig. 2 UV-vis spectra of $PMAA_{40}$-g-$PMOXA_6$ (a), $PMAA_{20}$-g-$PMOXA_6$ (b) and $PMAA_{20}$-g-$PMOXA_{12}$ (c) with dithiobenzoate groups (dash trace) and after treatment with MEA (solid trace).

shown in ESI (Table S1 and Fig. S2). The molecular weight distribution of the resulting copolymers was relatively low (PDI<1.3), demonstrating the good control of the polymerization. However, the tailing of the peaks illustrated there are some adsorption between copolymer and column.

The reduction of the terminal group of above copolymer was confirmed by NMR spectra and UV–vis spectra. It can be seen in Fig. 1(c), the disappearance of aromatic proton around 7.4−8.2 ppm in the copolymer indicated the success of the reduction process. As illustrated in Fig. 2, the dithiobenzoate group has a strong absorption band around 305 nm in dash trace in Fig. 2 a, b and c for $PMAA_{40}$-g-$PMOXA_6$, $PMAA_{20}$-g-$PMOXA_6$, and $PMAA_{20}$-g-$PMOXA_{12}$, respectively. After reduction with MEA, the adsorption bands disappeared, indicating that the dithiobenzoate group at the chain end of PMAA-g-PMOXA was removed (as shown in solid trace in Fig. 2 (a), (b) and (c)), yielding the copolymers terminated with a thiol group ((PMAA-g-PMOXA)-SH).

The characterization of polymer-modified SPR sensors

Electrochemical measurements

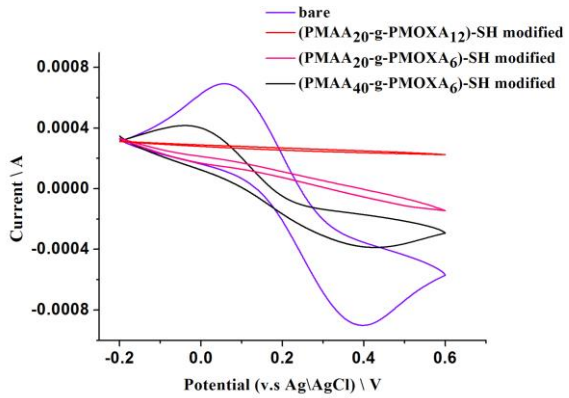

Fig. 3 Cyclic voltammograms for estimate the surface coverage of ($PMAA_{40}$-g-$PMOXA_6$)-SH (in black), ($PMAA_{20}$-g-$PMOXA_6$)-SH (in pink), ($PMAA_{20}$-g-$PMOXA_{12}$)-SH (in red) modified gold surface and bare gold surface (in purple).

The surface coverage of the modified gold sensors can be determined by cyclic voltammogram. Fig. 3 shows the CV curves of bare gold (in purple) sensor and ($PMAA_{40}$-g-$PMOXA_6$)-SH (in black), ($PMAA_{20}$-g-$PMOXA_6$)-SH (in pink) and ($PMAA_{20}$-g-$PMOXA_{12}$)-SH (in red) modified gold sensors. The bare gold sensor electrode reveals higher oxidation and reduction current peaks, indicating that the electron transfer reaction on the bare gold sensor surface was controlled by diffusion process. For ($PMAA_{20}$-g-$PMOXA_{12}$)-SH modified gold sensors, the CV shows the smallest oxidation and reduction current, which means ($PMAA_{20}$-g-$PMOXA_{12}$)-SH possessed the best blocking behavior for the electron transfer reaction. While in the case of ($PMAA_{20}$-g-$PMOXA_6$)-SH modified gold sensor, the CV also shows a good blocking behavior but no better than ($PMAA_{20}$-g-$PMOXA_{12}$)-SH modified gold sensors. Whereas the gold sensor modified with ($PMAA_{40}$-g-$PMOXA_6$)-SH exhibits a rather imperfect blocking behavior, in which charge can access and pass through the gold surface. This phenomenon closely relates to the surface coverage in which high surface coverage causes good blocking behavior.[45] Therefore, both ($PMAA_{20}$-g-$PMOXA_{12}$)-SH and ($PMAA_{20}$-g-$PMOXA_6$)-SH modified gold sensors showed high surface coverage, but the surface coverage of ($PMAA_{20}$-g-$PMOXA_{12}$)-SH with longer PMOXA chains was much higher than ($PMAA_{20}$-g-$PMOXA_6$)-SH with shorter PMOXA chains. This means the length of PMOXA side chains might influence the surface coverage of coating formed by (PMAA-g-PMOXA)-SH copolymer. Compared ($PMAA_{20}$-g-$PMOXA_6$)-SH modified gold sensor to ($PMAA_{40}$-g-$PMOXA_6$)-SH modified gold sensor, although the length of PMOXA side chains is the same in both copolymers, the surface coverage of theirs is different. The ($PMAA_{20}$-g-$PMOXA_6$)-SH with shorter PMAA backbone formed coating possessed much higher surface coverage than ($PMAA_{40}$-g-$PMOXA_6$)-SH with longer PMAA backbone. It is suggesting that the length of the PMAA backbone of (PMAA-g-PMOXA)-SH could affect the formation of the coating on the gold sensor, too much longer backbone will result in few polymers binding to the gold surface.

XPS measurements

In order to further characterize the modified gold sensors, the elemental composition of the ($PMAA_{40}$-g-$PMOXA_6$)-SH, ($PMAA_{20}$-g-$PMOXA_6$)-SH and ($PMAA_{20}$-g-$PMOXA_{12}$)-SH modified gold sensors and unmodified gold sensor was determined by XPS. As illustrated in Fig. 4(a), for the bare gold sensor surface (in black), Au element was detected and additional carbon and oxygen elements were also detected. The latter feature can be attributed to the unavoidable contamination of gold surfaces during preparation and analysis process. As for ($PMAA_{20}$-g-$PMOXA_{12}$)-SH modified gold surface (in red), the signals at 286.0, 400.1, 531.6 eV and 161.2 eV were ascribed to element C 1s, N 1s, O 1s and S 2p, respectively (Fig. 4(a)). Fig. 4(b) shows the enlarged S signal from ($PMAA_{20}$-g-$PMOXA_{12}$)-SH modified gold surface (Fig. 4(a)). S 2p at 161.2 eV was

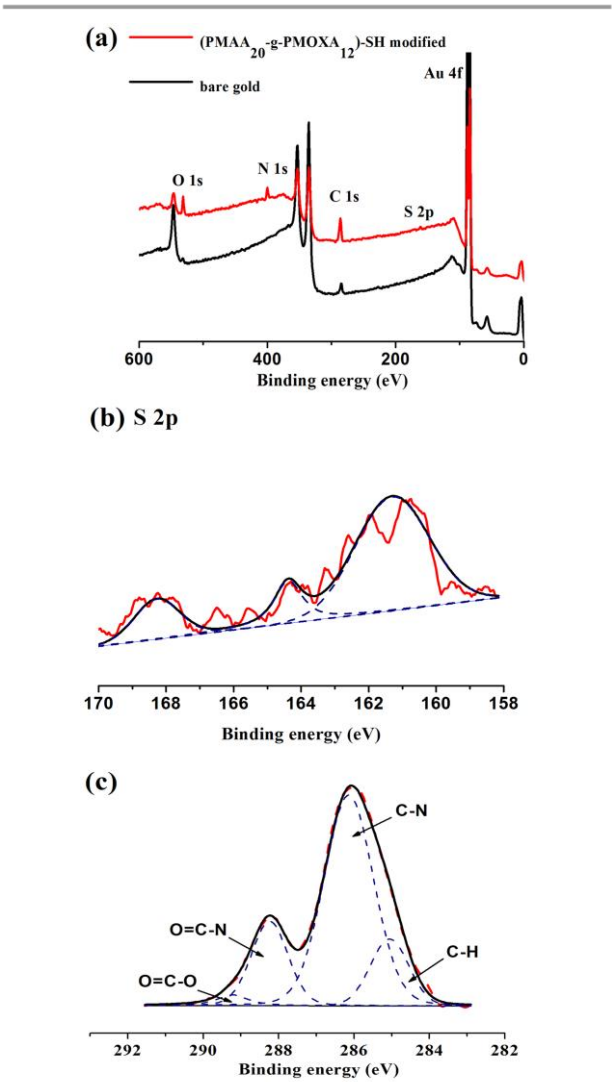

Fig 4 XPS spectra of wide scan for bare gold and ($PMAA_{20}$-g-$PMOXA_{12}$)-SH modified gold surface (a), the enlarged signal of S from ($PMAA_{20}$-g-$PMOXA_{12}$)-SH modified gold surface (b) and C 1s core-level spectra of the ($PMAA_{20}$-g-$PMOXA_{12}$)-SH modified gold surface (c).

Table 1. Atomic concentrations, static water contact angles and corresponding layer thickness of unmodified and bottle-brush polymer modified gold surfaces.

Surface	Atomic concentrations					Contact angle (deg)	Thickness (Å)
	Au(%)	C(%)	O(%)	N(%)	S(%)		
Bare gold	63.22	29.95	6.83			61±5	
($PMAA_{40}$-g-$PMOXA_6$)-SH modified	50.86	29.45	9.01	7.48	3.20	41±3	17.6±5.0
($PMAA_{20}$-g-$PMOXA_6$)-SH modified	32.38	41.32	13.69	9.36	3.25	28±3	46.0±6.0
($PMAA_{20}$-g-$PMOXA_{12}$)-SH modified	21.77	51.24	14.69	11.27	1.03	19±4	74.3±5.4

observed and indicated that the thiol was tethered covalently to the gold sensor; S 2p at 164.6 eV was also detected, which refer to the unbound thiol; another S 2p signal at 168.3 eV was due to the presence of oxidized sulfur species.[46] There were sharp increase in C 1s, N 1s, O 1s peaks' intensity and a decrease in Au 4f peak intensity for ($PMAA_{20}$-g-$PMOXA_{12}$)-SH modified gold surface compared to the bare gold surface. While in Fig 4(c), the XPS C 1s core-level spectra of ($PMAA_{20}$-g-$PMOXA_{12}$)-SH modified gold surface are curve-fitted into four peak components with binding energies at 284.7, 285.8, 287.7 and 288.6 eV, attributed to the C-H, C-N, O=C-N and O=C-O species, respectively. The appearance of the peak assigned to C–N bond at 285.8 eV is contributions from PMOXA. We also did the same XPS analysis for another two polymer coating surfaces. The XPS data are summarized in Table 1. For ($PMAA_{40}$-g-$PMOXA_6$)-SH modified gold surface, the Au signal was still large remained about 50.86%, with decreasing DP of backbone, for ($PMAA_{20}$-g-$PMOXA_6$)-SH modified gold surface, the atomic concentration of Au decreased from 50.86% to 32.38% and the atomic concentration of C, O and N increased from 29.45% to 41.32%, 9.01% to 13.69%, 7.48% to 9.36%, respectively. Obviously after decreasing the PMAA backbone length, the surface coverage was increased. It is noticed that ($PMAA_{20}$-g-$PMOXA_{12}$)-SH modified gold surface showed the least atomic concentration of Au and the highest atomic concentration of C, N, O, represented the best surface coverage of the three coatings. Compared $PMAA_{20}$-g-$PMOXA_{12}$)-SH modified gold surface with ($PMAA_{20}$-g-$PMOXA_6$)-SH modified gold surface, the XPS results suggested that increasing the PMOXA side chain length can also slightly increase the surface coverage. The XPS results are consistent with the above CV results. The atomic concentration of S in three coatings was slight higher for there might be a trace amount of sulfur-containing small molecule contaminants that cannot be completely removed in the modify process of sensors.[43]

Surface hydrophilicity and layer thickness

Static water contact angles were used to determine the hydrophilicity of the bottle-brush polymer modified gold sensors. From the results presented in Table 1, the water contact angle on the unmodified gold surface is 61±10 º. After modified with the ($PMAA_{40}$-g-$PMOXA_6$)-SH, （$PMAA_{20}$-g-$PMOXA_6$)-SH and （$PMAA_{20}$-g-$PMOXA_{12}$)-SH bottle-brush polymer, the water contact decreased to 41±3 º, 28±3 º, and 19±4 º, respectively. While the PMOXA unit was tethered to the gold surface, the water contact angle of gold surface decreased due to the excellent hydrophilicity of PMOXA. It can be seen that the（$PMAA_{20}$-g-$PMOXA_{12}$)-SH modified gold sensor showed the least contact angle, implying that this coating contained a maximum of PMOXA compared with other copolymers. This observation is in good agreement with the XPS results, in which it was found the amount of the hydrophilic PMOXA increased from ($PMAA_{40}$-g-$PMOXA_6$)-SH, to （$PMAA_{20}$-g-$PMOXA_6$)-SH and ($PMAA_{20}$-g-$PMOXA_{12}$)-SH modified surface. The dry thickness of the bottle-brush polymer layer on the gold surface was tested by ellipsometry. After three repeated experiments, we obtained a thickness about modified gold. The thickness of ($PMAA_{40}$-g-$PMOXA_6$)-SH modified gold was only 17.6±5.0 Å. This is due to the low surface coverage of ($PMAA_{40}$-g-$PMOXA_6$)-SH modified gold as determined by CV and XPS measurements. While for ($PMAA_{20}$-g-$PMOXA_6$)-SH modified surface, the film thickness increased to 46±6.0 Å. With decreasing the DP of the PMAA backbone, more bottle-brush polymer can bond to the gold surface, therefore the layer thickness was increased. And after modified using ($PMAA_{20}$-g-$PMOXA_{12}$)-SH, the film showed the largest thickness of 74.3±5.4 Å. It is obvious that the dry film thickness increased with increasing the surface

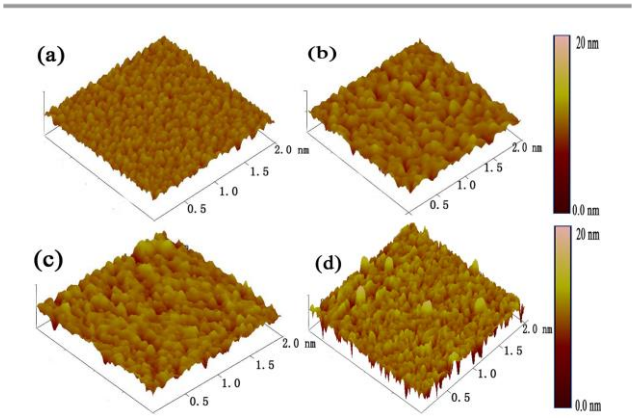

Fig. 5 AFM 3D images showing the surface morphology of: (a) unmodified gold surface, (b) ($PMAA_{40}$-g-$PMOXA_6$)-SH modified gold surface, (c) ($PMAA_{20}$-g-$PMOXA_6$)-SH modified gold surface, (d) ($PMAA_{20}$-g-$PMOXA_{12}$)-SH modified gold surface.

coverage.

AFM measurements

The morphologies of the unmodified gold and modified gold surfaces were investigated by AFM with tapping mode in dry state. A significant difference of surface morphologies between the unmodified and modified surfaces could be observed, which was also reflected by their root mean square (RMS) surface roughness values. As shown in the AFM images (Fig. 5), the bare gold surface was homogeneous and uniform, with RMS roughness of 1.23 nm (Fig. 5(a)). The RMS roughness was1.44 nm after modified with ($PMAA_{40}$-g-$PMOXA_6$)-SH (Fig. 5(b)). While the ($PMAA_{20}$-g-$PMOXA_6$)-SH modified gold had a value of 1.91 nm (Fig. 5(c)). As for the ($PMAA_{20}$-g-$PMOXA_{12}$)-SH modified gold surface, the RMS roughness increased to 2.71 (Fig. 5(d)). It can be seen that the bare gold surface showed homogeneous and small Au particles, while after modified with the ($PMAA_{40}$-g-$PMOXA_6$)-SH there were some nonuniform nano-islands. The phenomenon is closely related to the low surface coverage of ($PMAA_{40}$-g-$PMOXA_6$)-SH modified surface. The apparent increment in RMS roughness for ($PMAA_{20}$-g-$PMOXA_6$)-SH and ($PMAA_{20}$-g-$PMOXA_{12}$)-SH modified surfaces is owing to that with the increase of surface coverage, more extended structures were formed on ($PMAA_{20}$-g-$PMOXA_6$)-SH and ($PMAA_{20}$-g-$PMOXA_{12}$)-SH modified gold surfaces, thus the roughness is increased.[47]

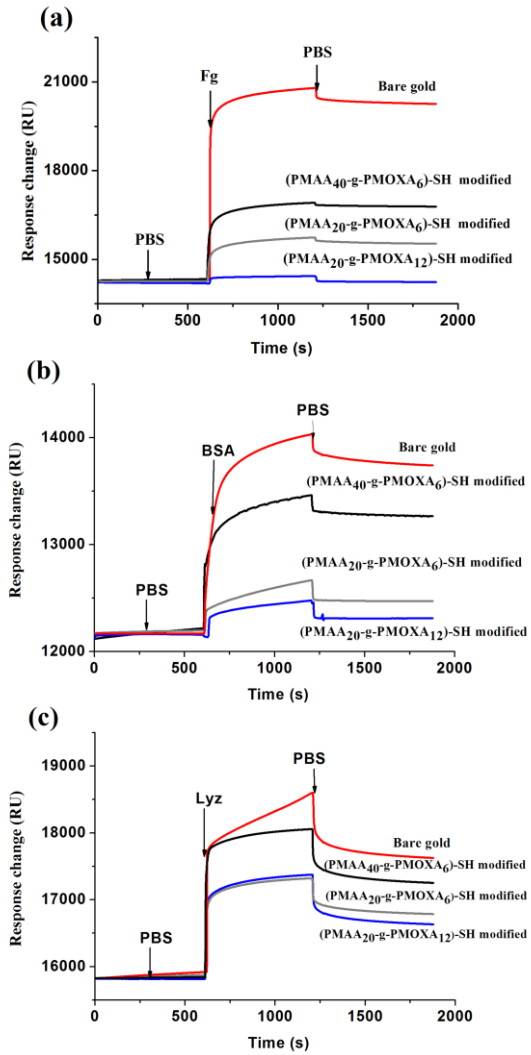

Fig. 6 Fouling from Fg (a), BSA (b) and Lyz (c) protein solution adsorption on unmodified and ($PMAA_{40}$-g-$PMOXA_6$)-SH, ($PMAA_{20}$-g-$PMOXA_6$)-SH and ($PMAA_{20}$-g-$PMOXA_{12}$)-SH modified gold surfaces, respectively.

The study of antifouling property

Protein resistant property

Three proteins Fg, BSA, Lyz were used in this experiment, because of their different molecule weight and isoelectric point. Fig 6 shows SPR profiles obtained for the adsorption of Fg (Fig. 6(a)), BSA (Fig. 6(b)) and Lyz (Fig. 6(c)) on ($PMAA_{40}$-g-$PMOXA_6$)-SH , ($PMAA_{20}$-g-$PMOXA_6$)-SH and ($PMAA_{20}$-g-$PMOXA_{12}$)-SH modified gold surface, as well as on bare gold surfaces. As shown in Fig. 6(a), Fg adsorbed strongly on the control bare gold surface, while after modified with ($PMAA_{40}$-g-$PMOXA_6$)-SH, ($PMAA_{20}$-g-$PMOXA_6$)-SH and ($PMAA_{20}$-g-$PMOXA_{12}$)-SH, the adsorbed mass decreased rapidly to a degree of approximately 61.3±1.3%, 78.2±4.4%, 96.5±3.1%, respectively. Fig. 6(b) shows the data for the adsorption of BSA on three polymer modified gold surface and on bare gold surface. We observed that ($PMAA_{40}$-g-$PMOXA_6$)-SH, ($PMAA_{20}$-g-$PMOXA_6$)-SH and ($PMAA_{20}$-g-$PMOXA_{12}$)-SH modified gold surface reduced the protein adsorption to 31.4±6.6%, 63.2±5.0%, 85.8±5.7%, respectively, as compared to the amount of protein adsorbed on bare gold surface. Similar results were obtained for Lyz adsorbed on ($PMAA_{40}$-g-$PMOXA_6$)-SH, ($PMAA_{20}$-g-$PMOXA_6$)-SH and ($PMAA_{20}$-g-$PMOXA_{12}$)-SH modified gold surface (Fig. 6(c)), the adsorption levels of Lyz decreased to 22.8±7.8%, 38.0±7.1%, 49.4±1.6%, respectively. After modified with bottle-brush polymers (PMAA-g-PMOXA)-SH, the gold surfaces have shown good performance for protein adsorption. In the recent study of our group[27], comb copolymers PMOXA-r-GMA coating formed on silicon/glass surfaces have also shown resistance to the adsorption of fluorescently labeled BSA. Therefore, we believe that PMOXA is a good candidate for the preparation of material with anti-protein adsorption property. As we can see from these results that the ($PMAA_{20}$-g-$PMOXA_{12}$)-SH modified gold showed the best protein resistant property obviously. It is generally accepted that surface packing density is critical factor for controlling nonspecific protein adsorption.[48] ($PMAA_{40}$-g-$PMOXA_6$)-SH with the lowest surface coverage resulted in highest protein adsorption. From the SPR results, we found that the adsorption of three proteins decreased with increasing surface coverage. To the best of our knowledge, the protein adsorption on surface also has a large relationship with the hydrophilicity and thickness of the binding polymer. ($PMAA_{20}$-g-$PMOXA_{12}$)-SH modified gold sensor showed better hydrophilicity and thicker thickness, resulting in better protein resistant property. Recently, Zhang and coworkers[36] found the side chain length of bottle-brush brushes have a significant influence on protein adsorption that sufficient side chain length (DP>10) tend to

provide a very low protein adsorption. In our study, the similar phenomena were observed that ($PMAA_{20}$-g-$PMOXA_{12}$)-SH coating (DP > 10) with longer side chains exhibited better protein resistant property than the（$PMAA_{20}$-g-$PMOXA_6$)-SH coating with short side chains (DP < 10). Also, they found poly(2-methyl-2-oxazoline) based bottle-brush brushes modified silicon substrate possessed extremely low protein adsorption property (fluorescent labeled fibronectin adsorption ≤ 6 ng/cm^2). Our studies also indicated that bottle-brush brushes ($PMAA_{20}$-g-$PMOXA_{12}$)-SH modified gold substrate prepared by "grafting to" method also revealed a good protein resistant property. All of three coatings showed the similar phenomena that the reduced level of Lyz adsorption was lower while compared with Fg and BSA. Another factor, the electrostatic interactions should be taken into account. Under the measurement conditions, residues COO^- in polymer keep negatively charged, thus it will adsorb positively charged proteins like Lyz, and repel negatively charged proteins like Fg and BSA.

Platelet adhesion

In order to determine the potential blood compatibility of the unmodified and modified gold surfaces, platelet adhesion studies were also conducted, since platelet adhesion is one of the most important steps during blood coagulation. For the platelet adhesion studies, PRP separated from the blood of a healthy human was incubated on unmodified and modified gold sensors. It can be seen from Fig. 7(a) (with a magnification of 3000) that massive platelets adhered and aggregated on the unmodified gold surface. After modified with ($PMAA_{40}$-g-$PMOXA_6$)-SH (Fig. 7(b)), there were still several platelets on the surface. While the gold surface was modified with ($PMAA_{20}$-g-$PMOXA_6$)-SH (Fig. 7(c)), a dramatic reduction in platelet adhesion was observed. As for the ($PMAA_{20}$-g-$PMOXA_{12}$)-SH modified gold surface (Fig. 7(d)), there was almost no platelet adhering. The results of the platelet adhesion are consistent with the results of protein adsorption, in which ($PMAA_{20}$-g-$PMOXA_{12}$)-SH modified gold surface showed the best protein resistant property. The probable explanation could be addressed to this phenomenon. ($PMAA_{20}$-g-$PMOXA_{12}$)-SH modified gold surface with the best surface hydrophilicity tend to form a hydration layer on the surface, therefore the energy barrier that has to be overcome to disrupt the hydration makes the adsorbing of protein or platelet energetically less favorable. Previous study in our group[27] testified that comb copolymers PMOXA-r-GMA coating formed on silicon/glass surfaces also exhibited an excellent resistance to platelet adhesion. All above results elucidated that PMOXA can be considered as a basic unit for the preparation of antifouling material with different structure.

Conclusions

In summary, this work demonstrated a feasible and convenient method to fabricate a protein resistant coating on gold surface. A series of well-controlled bottle-brush polymers (PMAA-g-PMOXA) were synthesized by RAFT polymerization and CROP. And then the monothiol-terminated bottle-brush (PMAA-g-PMOXA)-SH were grafted to the surface of gold sensors in situ aminolysis reaction. The bottle-brush coating exhibited a good property of protein resistance and anti-platelet adhesion, compared to the bare gold sensor. Furthermore, the antifouling properties of polymers on the gold surface were optimized by adjusting the bottle-brush architecture. Compared ($PMAA_{20}$-g-$PMOXA_6$)-SH coating to ($PMAA_{40}$-g-$PMOXA_6$)-SH coating we found that the backbone length may influence the surface coverage based on this method determined by XPS and CV measurements. The results of ($PMAA_{20}$-g-$PMOXA_{12}$)-SH coating and（$PMAA_{20}$-g-$PMOXA_6$)-SH coating clearly showed a correlation between the side chain length and antifouling property, ($PMAA_{20}$-g-$PMOXA_{12}$)-SH with the longer hydrophilic segment resulting in more hydrophilicity coating surface and better antifouling property proved by CA, SPR and platelet adhesion experiments. Overall, this method will be useful for fabricate antifouling gold surfaces with potential applications in biosensor and biomedical areas.

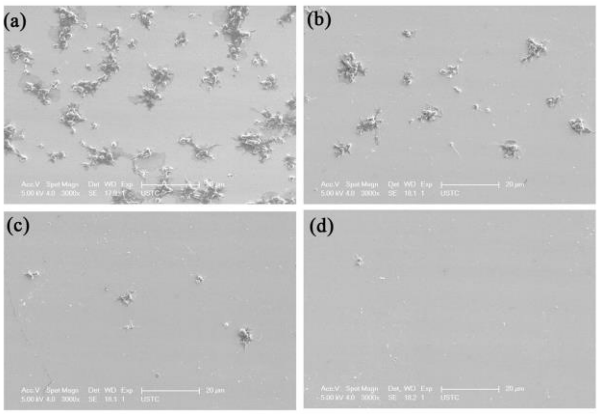

Fig. 7 SEM images of the adhesion of blood platelets on unmodified gold surface (a) and ($PMAA_{40}$-g-$PMOXA_6$)-SH (b), ($PMAA_{20}$-g-$PMOXA_6$)-SH (c), ($PMAA_{20}$-g-$PMOXA_{12}$)-SH (d) modified gold surfaces, respectively.

Acknowledgements

This work was supported by the National Natural Science Foundation of China under Grant No. 21374109, and Ministry of Science and Technology of China under Grant No. 2012CB933802.

Notes and references

1 C. Fang, N. M. Bandaru, A. V. Ellis and N. H. Voelcker, *J. Mater. Chem.*, 2012, **22**, 2952-2957.
2 M. Couture, S. S. Zhao and J.-F. Masson, *Phys. Chem. Chem. Phys.*, 2013, **15**, 11190-11216.
3 T. Shahal, K. A. Melzak, C. R. Lowe and E. Gizeli, *Langmuir*, 2008, **24**, 11268-11275.
4. R. Bordes, J. r. Tropsch and K. Holmberg, *Langmuir*, 2010, **26**, 10935-10942.
5 X. Ye, X. Jiang, B. Yu, J. Yin and P. Vana, *Biomacromolecules*, 2012, **13**, 535-541.

6 L. M. Feller, S. Cerritelli, M. Textor, J. A. Hubbell and S. G. Tosatti, *Macromolecules*, 2005, **38**, 10503-10510.
7 J. Bearinger, S. Terrettaz, R. Michel, N. Tirelli, H. Vogel, M. Textor and J. Hubbell, *Nat. Mater.*, 2003, **2**, 259-264.
8 J. C. Love, L. A. Estroff, J. K. Kriebel, R. G. Nuzzo and G. M. Whitesides, *Chem. Rev.*, 2005, **105**, 1103-1170.
9 R. B. Belshe, *New Engl. J. Me*d., 2005, **353**, 2209-2211.
10 H.-M. So, K. Won, Y. H. Kim, B.-K. Kim, B. H. Ryu, P. S. Na, H. Kim and J.-O. Lee, *J. Am. Chem. Soc.*, 2005, **127**, 11906-11907.
11 M. J. Barry, *New Engl. J .Med.*, 2001, **344**, 1373-1377.
12 G. B. Sigal, M. Mrksich and G. M. Whitesides, *J. Am. Chem. Soc.*, 1998, **120**, 3464-3473.
13 S. R. Benhabbour, L. Liu, H. Sheardown and A. Adronov, *Macromolecules*, 2008, **41**, 2567-2576.
14 L. D. Unsworth, H. Sheardown and J. L. Brash, *Langmuir*, 2005, **21**, 1036-1041.
15 J.-F. Masson, T. M. Battaglia, M. J. Davidson, Y.-C. Kim, A. Prakash, S. Beaudoin and K. S. Booksh, *Talanta*, 2005, **67**, 918-925.
16 J.-F. Masson, T. M. Battaglia, Y.-C. Kim, A. Prakash, S. Beaudoin and K. S. Booksh, *Talanta*, 2004, **64**, 716-725.
17. H. M. Zareie, C. Boyer, V. Bulmus, E. Nateghi and T. P. Davis, *Acs Nano*, 2008, **2**, 757-765.
18 S. Liu, L. Chen, L. Tan, F. Cao, L. Bai and Y. Wang, *J. Mater. Chem. B*, 2014, **2**, 6758-6766.
19 O. Pop-Georgievski, C. Rodriguez-Emmenegger, A. de los Santos Pereira, V. Proks, E. Brynda and F. Rypáček, *J. Mater. Chem. B*, 2013, **1**, 2859-2867.
20. R. D. Dabholkar, R. M. Sawant, D. A. Mongayt, P. V. Devarajan and V. P. Torchilin, *Int. J. Pharm.*, 2006, **315**, 148-157.
21 M. Shen, L. Martinson, M. S. Wagner, D. G. Castner, B. D. Ratner and T. A. Horbett, *Journal of Biomaterials Science*, Polymer Edition, 2002, **13**, 367-390.
22 D. W. Branch, B. C. Wheeler, G. J. Brewer and D. E. Leckband, *Biomaterials*, 2001, **22**, 1035-1047.
23 B. Pidhatika, J. Möller, E. M. Benetti, R. Konradi, E. Rakhmatullina, A. Mühlebach, R. Zimmermann, C. Werner, V. Vogel and M. Textor, *Biomaterials*, 2010, **31**, 9462-9472.
24 F. Wiesbrock, R. Hoogenboom, M. A. Leenen, M. A. Meier and U. S. Schubert, *Macromolecules*, 2005, **38**, 5025-5034.
25 P. Brož, S. M. Benito, C. Saw, P. Burger, H. Heider, M. Pfisterer, S. Marsch, W. Meier and P. Hunziker, *J. Control Release*, 2005, **102**, 475-488.
26 R. Konradi, B. Pidhatika, A. Mühlebach and M. Textor, *Langmuir*, 2008, **24**, 613-616.
27 L. Bai, L. Tan and S. Liu, Y. Wang. *J. Mater. Chem. B*, 2014, **2**, 7785-7794.
28 L. Barner, *Adv. Mater.*, 2009, **21**, 2547-2553.
29 L.-N. Xiang, L.-J. Chen, L. Tan, C. Zhang, F.-H. Cao, S.-T. Liu and Y.-M. Wang, *Chinese Chem. Lett.*, 2013, **24**, 597-600.
30 S. Le-Masurier, G. Gody, S. Perrier and A. Granville, *Polym. Chem.*, 2014, **5**, 2816-2823.
31 W. Li, C. Bao, R. A. Wright and B. Zhao, *Rsc Adv.*, 2014, **4**, 18772-18781.
32 F. He, B. Luo, S. Yuan, B. Liang, C. Choong and S. O. Pehkonen, *Rsc Adv.*, 2014, **4**, 105-117.
33 X. Li, S. L. Prukop, S. L. Biswal and R. Verduzco, *Macromolecules*, 2012, **45**, 7118-7127.
34 S. Krishnan, C. J. Weinman and C. K. Ober, *J. Mater. Chem.*, 2008, **18**, 3405-3413.
35 A. Rosenhahn, S. Schilp, H. J. Kreuzer and M. Grunze, *Phys. Chem. Chem. Phys.*, 2010, **12**, 4275-4286.
36 N. Zhang, T. Pompe, I. Amin, R. Luxenhofer, C. Werner and R. Jordan, *Macromol. Biosci.*, 2012, **12**, 926-936.
37 C. Weber, C. Remzi Becer, W. Guenther, R. Hoogenboom and U. S. Schubert, *Macromolecules*, 2009, **43**, 160-167.
38 M. Citartan, S. C. Gopinath, J. Tominaga, Y. Chen and T.-H. Tang, *Talanta*, 2014, **126**, 103-109.
39 S.-H. Hsu, D. N. Reinhoudt, J. Huskens and A. H. Velders, *J. Mater. Chem.*, 2011, **21**, 2428-2444.
40 M. Nakayama and T. Okano, *Biomacromolecules*, 2005, **6**, 2320-2327.
41 Z. Wang, J. He, Y. Tao, L. Yang, H. Jiang and Y. Yang, *Macromolecules*, 2003, **36,** 7446-7452.
42 P. J. Roth, D. Kessler, R. Zentel and P. Theato, *Macromolecules*, 2008, **41**, 8316-8319.
43 P. Akkahat, S. Kiatkamjornwong, S.-i. Yusa, V. P. Hoven and Y. Iwasaki, *Langmuir*, 2012, **28**, 5872-5881.
44 S. Perrier, C. Barner-Kowollik, J. F. Quinn, P. Vana and T. P. Davis, *Macromolecules*, 2002, **35**, 8300-8306.
45 V. Ganesh, S. K. Pal, S. Kumar and V. Lakshminarayanan, J. *Colloid Interf. Sci.*, 2006, **296**, 195-203.
46 D. G. Castner, K. Hinds and D. W. Grainger, *Langmuir*, 1996, **12**, 5083-5086.
47 Y. Zhuang, Q. Zhu, C. Tu, D. Wang, J. Wu, Y. Xia, G. Tong, L. He, B. Zhu and D. Yan, *J. Mater. Chem.*, 2012, **22**, 23852-23860.
48 S. Herrwerth, W. Eck, S. Reinhardt and M. Grunze, *J. Am. Chem. Soc.*, 2003, **125**, 9359-9366.